

PROMPT FISSION NEUTRON DATA

Horst Märten, Dietmar Richter, Andreas Ruben, and Dieter Seeliger

Technische Universität Dresden
MommSENstrasse 13, DDR-8027 Dresden, G.D.R.

Waldemar Neubert

Central Institute for Nuclear Research, Rossendorf
PF 19, DDR-8051 Dresden, G.D.R.

Albert Lajtai

Central Research Institute for Physics, Budapest
POB 49, H-1525 Budapest, Hungary

Abstract: The energy and angular distribution of prompt neutrons from ^{252}Cf spontaneous fission has been measured by the use of direction-sensitive fragment spectroscopy in conjunction with neutron time-of-flight spectroscopy. These data covering the whole angular range from 0° to 180° and the energy range from 100 keV to 10 MeV (18 MeV in polar direction) were the basis for the test of complex statistical-model approaches to prompt fission neutron emission.

Calculations have been performed in the framework of the cascade evaporation model (CEM) as well as the generalized Madland-Nix model (GMNM).

Using the parameter-free CEM several global methods for the description of optical potential and nuclear level density have been studied. The combination of the GMNM, whose free parameters were adjusted to reproduce the measured Cf data, with a simple scission point model including semi-empirical, temperature-dependent shell correction energies provide the basis for the consistent description of fragment energies (kinetic energy, excitation energy), prompt-neutron yields, energy and angular distributions of prompt fission neutrons as a function of mass asymmetry for any induced fission reaction in the Th-Cf region including the separate consideration of multiple-chance fission at high incidence energy.

(fission reactions, neutron energy spectra, fission neutron multiplicity, statistical model, fission theory, nuclear data evaluation)

Introduction

Many microscopic measurements of energy and angular distributions have shown that prompt fission neutrons (PFN) are predominantly evaporated from highly excited and rapidly moving fragments. PFN energy spectra have been mostly described phenomenologically by either a Maxwellian or a Watt distribution /1,2/. However, theoretical approaches needed for the physically consistent description of PFN data should account for the complexity of PFN emission, i.e. the cascade-like evaporation from a fragment diversity characterized by an occurrence probability distribution $P(\{p_f\})$ ($\{p_f\}$ - fragment parameter set, e.g. A - mass number, Z - charge number, TKE - total kinetic energy, E^* - excitation energy, I - angular momentum) /3,4/. In general, PFN emission has to be understood as a superposition of different components corresponding to specific mechanisms. In addition to the main one, i.e. evaporation from fully accelerated fragments, the so-called "scission neutron" emission due to rapid nuclear-potential changes close to scission, the PFN emission during fragment acceleration (probably including non-equilibrium effects), and neutron emission from n-unstable

light charged particles as 5-He and 6-He after ternary fission can be assumed /5/. The possible role of secondary mechanisms has been studied in several works cited and discussed in Ref. 5. The main source of some contradictions is probably the non-adequate theoretical description of the predominant mechanism. The present work represents results of recent experimental and theoretical studies. Further, the theoretical concept for the calculation of PFN data for any fission reaction is formulated. It is based on a generalization of the Madland-Nix model /6,7/ and includes semi-empirical theoretical approaches to predict the relevant $P(\{p_f\})$ distribution.

Fundamental Investigations of PFN Emission

Experiment

Previous measurements of the emission probability $N(E,\theta)$, where E and θ are the PFN energy and angle with reference to light-fragment direction, respectively, were mostly based on fragment spectroscopy for a fixed solid angle and the consecutive measurement of neutron spectra at selected neutron detector positions (e.g. Ref. 8). The method used in this work relies on the direction-sensitive spectroscopy of fragments

(combination of a single and position-sensitive parallel-plate avalanche counter) in combination with neutron time-of-flight spectroscopy applying two neutron detectors (NE 213 liquid scintillator for medium and high energy, NE 912 6-Li glass scintillator for low-energy range) at fixed position. Details of this arrangement as well as the data analysis have been described in Ref. 9. The data measured cover the full angle range (0-180 deg) and the 100 keV - 10 MeV (18 MeV in polar direction) energy range. The experimental results are in good agreement with recent data measured by Knitter and Budtz-Jorgensen /10/, but exhibit remarkable contradictions to earlier results of Bowman et al. /8/ at equatorial direction ($\theta = 90$ deg), in particular at high energy.

Statistical-Model Approach

The cascade evaporation model (CEM) /3/ is assumed to provide the basis for an adequate description of the main PFN component, i.e. evaporation from fully accelerated fragments. The CEM which incorporates an extended Weisskopf ansatz /11/ accounts for

- (i) a complex fragment distribution $P(\{A, TKE, E^*\}, \bar{Z}(A), \bar{I}(A))$,
- (ii) cascade emission,
- (iii) neutron- γ -competition of prompt fragment de-excitation
- (iv) emission anisotropy in the centre-of-mass system (CMS) due to fragment angular momentum $\bar{I}(A)$ according to a semiclassical approach /12/,
- (v) semi-empirical description of level density considering shell and pairing effects,
- (vi) optical-model (OM) cross section for compound-nucleus formation calculated on the basis of global OM potentials,
- (vii) exact transformation of the CMS distributions into the laboratory system (LS) /3,5/.

The CEM has been successfully applied to reproduce the standard neutron spectrum from $^{252}\text{Cf}(sf)$ in a wide energy range /13/. The CEM version used in this work has been extended concerning the items (iii), (iv), and (vi) to describe the $N(E, \theta)$ data in the full co-ordinate range, in particular in the crucial polar regions at E close to the fragment kinetic energy per nucleon, i.e. at very low CMS energy (singular point of CMS-LS transformation) /4/.

Results

Differential PFN spectra at both polar as well as at equatorial direction, which are very sensitive concerning the study of emission mechanisms, are represented in Figs. 1 and 2. The results show the strong influence of the chosen OM potential on the calculated PFN distribution in the crucial regions discussed above.

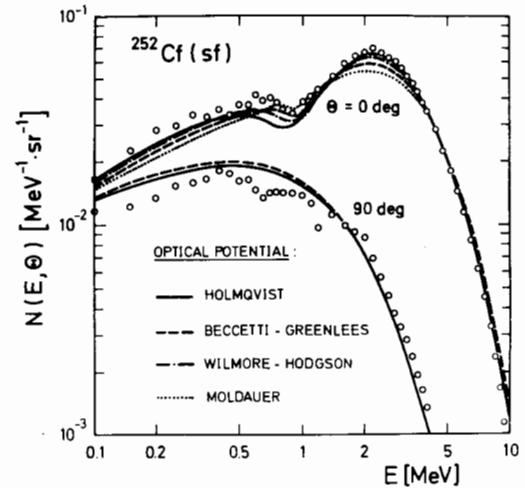


Fig. 1 Differential PFN spectra for 0 and 90 deg. Experimental data (circles) are shown in comparison with CEM results obtained by the use of several OM potentials as indicated.

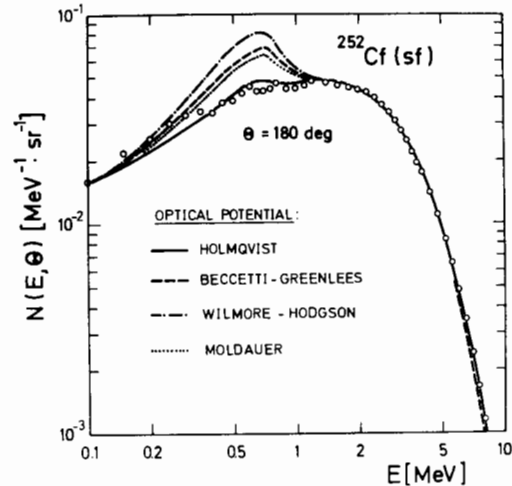


Fig. 2 As for Fig. 1, but for $\theta = 180$ deg

In summary, the CEM reproduces experimental PFN data (cf. Ref. 4). There is no significant indication of secondary mechanisms of PFN emission in contrast to several previous works, e.g. Ref. 8, based on rather rough theoretical approaches combined with parameter adjustments. Note that the CEM is parameter-free. Considering experimental as well as theoretical uncertainties the upper limit of the yield of secondary PFN has been estimated to be about 5%. This result justifies the alone consideration of the predominant mechanism of PFN emission for practical calculations. However, the CEM cannot be easily applied to any fission reaction due to the lack of knowledge of $P(\{p_f\})$. Fundamental fission theories fail to reproduce $P(\{p_f\})$ completely and/or with sufficient accuracy. Therefore, the following theoretical concept is proposed for practical considerations.

Calculation of PFN Data for Applied Purposes

Generalized Madland-Nix Model (GMNM)

Compared with CEM, the GMNM /7/ is a simplified approach. However, the most important characteristics of PFN emission are taken into account:

- (i) approximative consideration of fragment distribution in E^* and cascade emission /6/,
- (ii) inclusion of PFN spectrum dependence on A /7/,
- (iii) CMS anisotropy of PFN emission,
- (iv) simulation of neutron- γ -competition by introducing a lower limit T_0 of integration over rest-nucleus temperature T .

Based on $\bar{E}^*(A)$, $\overline{TK\bar{E}}(A)$, $Y(A)$ (fragment mass yield) and $W_{ff}(\bar{\theta})$ (fragment angular distribution with reference to incidence-beam direction), the GMNM provides the following results: neutron yield $\bar{v}(A)$, $N(E, \theta)$, $N(E)$, and $N(E, \Psi)$, where Ψ is the PFN angle with reference to incidence-beam direction. Both free parameters of the GMNM (scaling factor of level density parameter $a(A)$, T_0) have been adjusted on the basis of $^{252}\text{Cf}(sf)$ data.

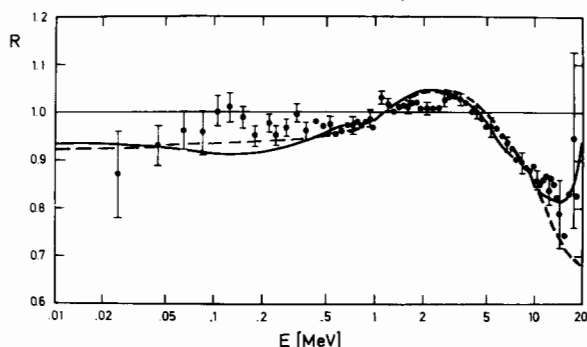


Fig. 3 ^{252}Cf PFN spectrum represented as ratio to Maxwellian with $T_M=1.42$ MeV: dots - evaluation /14/, — CEM, --- GMNM.

Thus, the accuracy of GMNM calculations is comparable with CEM. However, GMNM applications require the knowledge of the input data stated above.

Semi-empirical Fission Theories

A simple scission point model /20/ is applied to solve the energy partition problem, i.e. to deduce $\overline{TK\bar{E}}(A)$ and $\bar{E}^*(A)$ (two-spheroid model TSM).

It includes semi-empirical shell correction energies depending on scission point temperature.

A generalized version of the 5-Gaussian approach to fragment mass yields $Y(A)$ /15/ is used for the calculations.

Angular distributions of fission fragments are deduced within the statistical model /16/.

All these semi-empirical approaches can be applied to any fission reactions in the Th-Am region for excitation energies of the fissioning nucleus below ~ 25 MeV.

Multiple-Chance Fission

In case of rather high incidence

energy, multiple-chance fission reactions are considered separately for all possible chances in conjunction with the statistical-model analysis of the partial fission cross sections and scattered-neutron as well as γ -ray cross sections (code STAPRE /17/ with fission channel, cf. Ref. 18). Accordingly, the GMNM calculations are carried out for each chance. This general approach provides the basis for a physically consistent calculation of PFN data, fragment data, and reaction cross sections.

Selected Results

It has been shown recently that the GMNM-TSM combination yields PFN spectra for (n, f) reactions, which are in good agreement with experimental data /4/.

Fig. 4 represents results of PFN yields as function of neutron incidence energy for ^{232}Th and ^{238}U including multiple-chance fission region.

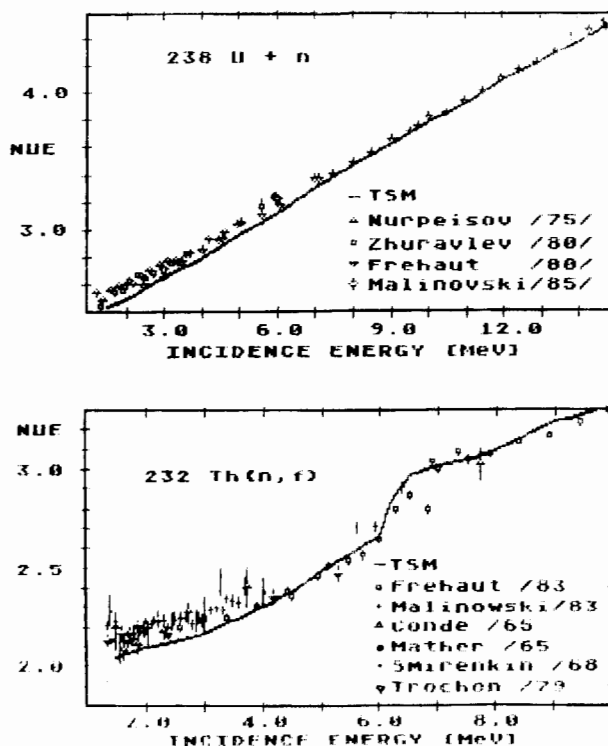


Fig. 4 Average PFN yield as function of neutron incidence energy: Experimental and evaluated data /CINDA-Catalogue/ in comparison with the calculation based on TSM-GMNM.

The calculations have been performed without data adjustments. The trend of the data is reproduced, in particular the step-like behaviour of $\bar{v}(E_n)$ at the $(n, n'f)$ threshold for ^{232}Th .

The correlation of \bar{v} and \bar{E} , i.e. the average LS PFN energy, is of high importance for practical considerations. In most cases, Terrell's relation /2/ is used. However, systematic deviations have been pointed out by Knitter et al. /19/. Fig. 5 shows the results of our calculations for pure (n, f) reactions. It is indicated that Terrell's original relation is not confirmed. The $\bar{E}(\bar{v})$ correlation is not unique for all fission

reactions considered. Hence, the separate theoretical analysis is necessary.

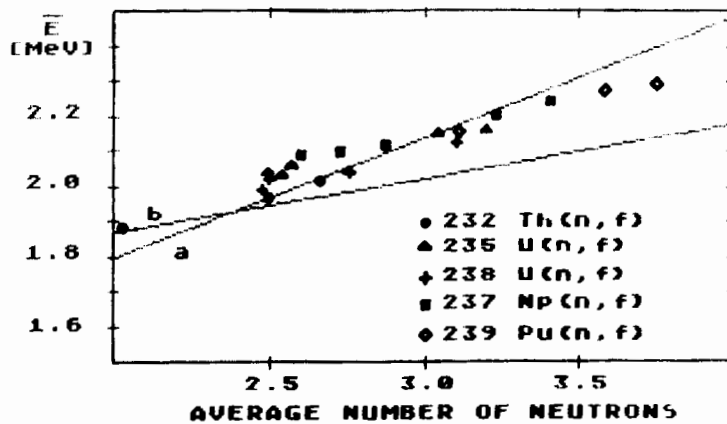


Fig. 5
The average LS PFN energy versus neutron multiplicity. Data points represents the results of GMNM calculations (a - Ref. 19, b - Ref. 1)

Conclusions

- (i) Experimental $N(E, \theta)$ data for $^{252}\text{Cf}(sf)$ are well reproduced by calculations in the framework of a complex statistical-model approach based on the assumption that all neutrons are evaporated from fully accelerated fragments.
- (ii) Complex calculations of PFN data for any fission reaction require the application of fission theory to describe the fragment occurrence probability $P\{p_f\}$. However, basic fission theories fail to describe fragment data with sufficient accuracy. Semi-empirical fission theories serve as alternative.
- (iii) PFN data calculations for multiple-chance fission have to be additionally connected with reaction theory to describe scattered-neutron spectra, partial fission cross sections, fragment data, and PFN data in a physically consistent manner.
- (iv) The TUD concept presented is applicable to fission reactions in the Th-Am region for neutron incidence energies lower than 20 MeV. It includes a complex statistical-model approach to PFN emission (GMNM).

REFERENCES

1. B.E. Watt: Phys.Rev. 87, 1037 (1952)
2. J. Terrell: Phys.Rev. 113, 527 (1959)
3. H. Märten and D. Seeliger: J.Phys. G10, 349 (1984)
4. H. Märten et al.: Proc.Int.Conf. on Neutron Physics, Kiev, 1987, in print
5. H. Märten et al.: Proc.Int.Conf. on Nucl.Phys. - Nuclear Fission -, Gaussig, 1985, ZfK-592, 1 (1986)
6. D.G. Madland and J.R. Nix: Nucl.Sci.Eng. 81, 213 (1982)
7. H. Märten and D. Seeliger: Nucl.Sci.Eng. 93, 370 (1986)
8. H.R. Bowman et al.: Phys.Rev. 126, 2120 (1962)
9. H. Märten et al.: Nucl.Instr.Meth. A264, 375 (1988); Rad.Eff. 93, 41 (1986)
10. C. Budtz-Jorgensen and H.H. Knitter: Rad. Eff. 93, 5 (1986)
11. J.M. Blatt and V.F. Weisskopf: Theoretical Nuclear Physics (New York, 1952)
12. T. Ericson and V. Strutinski: Nucl.Phys. 8, L 84 (1958)
13. H. Märten and D. Seeliger: Rad. Eff. 93, 99 (1986)
14. W. Mannhart: IAEA-TECDOC-410, 158 (1986)
15. C.A. Straede: Thesis, CBNM Geel, Belgium (1985)
16. J.R. Huizenga and R. Vandenbosch: Nuclear Reactions II (1962)
17. M. Uhl: Proc. Int.Conf.Nucl.Phys., Gaussig, 1982, ZfK-491, 155 (1982)
18. A.V. Ignatyuk et al.: Yad.Fiz. 47, 355 (1988)
19. H.H. Knitter et al.: Prompt Fission Neutron Spectra, Proc. IAEA Consultants' Meeting, Vienna, 1971 (IAEA, Vienna, 1972), 41
20. H. Märten et al.: Proc. Int. Conf. on Nucl. Phys., Gaussig, 1986, ZfK-610, 169 (1986)